

## Levels in $^{205}\text{Pb}$ Populated by the Decay of $^{205}\text{Bi}$

J. H. Hamilton, V. Ananthakrishnan, A. V. Ramayya, and W. M. LaCasse  
*Physics Department,\* Vanderbilt University, Nashville, Tennessee 37235*

and

D. C. Camp  
*Lawrence Livermore Laboratory,† Livermore, California 94550*

and

J. J. Pinajian and L. H. Kern  
*Oak Ridge National Laboratory,‡ Oak Ridge, Tennessee 37830*

and

J. C. Manthuruthil  
*Aerospace Research Laboratories, Wright-Patterson Air Force Base, Ohio 45433*

(Received 24 April 1972)

Chemically and isotopically separated sources of  $^{205}\text{Bi}$  were used to study the level structure of  $^{205}\text{Pb}$ .  $\gamma$ -ray data were taken with Ge(Li) detectors in the singles mode, with a Compton suppression spectrometer, and with a Ge(Li)-Ge(Li) two-parameter analyzer system in a  $4096 \times 2048$  coincidence mode. Conversion-electron data were taken with a Si(Li) detector. From these data 146 transitions were identified in the decay of  $^{205}\text{Bi}$ , and 130 were placed in a level scheme which included 26 definite and 1 tentatively assigned levels. Previously suggested levels at 1575.26, 1705.03, 1965.9, and 2521.40 keV were confirmed from coincidence data, while a 1129.9-keV level was not. New levels at 1756.4 and 1842.01 are established and an 1818-keV level tentatively assigned. Several new spin and parity assignments are made. Experimental results are compared with recent shell-model calculations.

### I. INTRODUCTION

The level structures of the lead isotopes have been of particular interest because they offer the opportunity to study single-particle orbitals in nuclei with one, two, three, or several particles or particle holes outside doubly magic  $^{208}\text{Pb}$ . Recently we initiated a program to systematically study the levels in the lead isotopes lighter than  $^{208}\text{Pb}$  from the decay of their bismuth parents. While extensive conversion-electron and some NaI(Tl)  $\gamma$ -ray spectra had been done, as summarized in the *Table of Isotopes*,<sup>1</sup> large Ge(Li) detectors used in singles and coincidence modes should reveal new features of the level structures of these nuclei. Work on the  $^{206}\text{Bi}$  decay was carried out first.<sup>2</sup> Here we report on studies in  $^{205}\text{Bi}$ . After our work was completed,<sup>3</sup> we learned of recent work by Rupp and Vegors<sup>4</sup> with Ge(Li) detectors in the single mode and Ge(Li)-NaI coincidence work. Their work indeed revealed many new features of this level structure. Our work included  $\gamma$ -ray singles studies with larger Ge(Li) detectors and with a Compton suppression system, conversion-electron measurements, and  $\gamma$ - $\gamma$  coincidence work with two large Ge(Li) detectors operated in

a  $4096 \times 2048$  mode. Our more extensive singles and coincidence data revealed the presence of many new transitions and additional levels which are reported here.

### II. EXPERIMENTAL TECHNIQUES

The 15.31-day  $^{205}\text{Bi}$  was prepared by irradiating 0.029-in. foils of radiogenic lead (obtained from the National Lead Company with an isotopic mass analysis of  $^{204}\text{Pb} < 0.10\%$ ,  $^{206}\text{Pb} 88.59\%$ ,  $^{207}\text{Pb} 8.36\%$ , and  $^{208}\text{Pb} 3.05\%$ ) for 4 h with  $\sim 18.5$ -MeV protons using a  $26.7$ - $\mu\text{A}$  beam current of the Oak Ridge National Laboratory 86-in. cyclotron. At this incident energy  $^{205}\text{Bi}$  is formed primarily by the reaction  $^{208}\text{Pb}(p, 2n)^{205}\text{Bi}$  ( $Q = -11.57$  MeV). In addition, varying amounts of 11.8-h  $^{203}\text{Bi}$ , 11.3-h  $^{204}\text{Bi}$ , and 6.24-day  $^{206}\text{Bi}$  plus a negligible amount of 30-yr  $^{207}\text{Bi}$  are formed. By allowing the sample to "cool" for  $\sim 100$  days, only the 15.3-day  $^{205}\text{Bi}$  remained with traces of 6.24-day  $^{206}\text{Bi}$ . The lead strip was dissolved in warm nitric acid and, after reducing the volume of the solution, the lead was precipitated from chilled fuming nitric acid. The precipitate was dissolved in dilute nitric acid, the pH was adjusted, and the bismuth

activity was extracted with dithizone solution. After traces of lead were washed out of the dithizone, the solution was evaporated down to dryness, treated with nitric acid to destroy organic material, and taken up in dilute nitric acid. Further reduction of solids was accomplished by adding  $\text{Fe}^{+++}$  carrier and coprecipitating bismuth with  $\text{Fe}(\text{OH})_3$  a number of times. The iron was subsequently removed by extraction with methyl isobutyl ketone (4-methyl-2-pentanone). The aqueous phase containing the bismuth activity was treated with nitric acid to destroy organic material and then taken up in dilute hydrochloric acid.

Additional sources of  $^{205}\text{Bi}$  were prepared by isotopic separation of chemically isolated  $^{205,206}\text{Bi}$  activity produced by the ( $p, xn$ ) reaction on natural lead. These sources are described elsewhere.<sup>2</sup> The isotopically separated source material was divided for spectroscopic studies at Vanderbilt and Livermore.

At Vanderbilt,  $\gamma$ -ray and conversion-electron singles studies were carried out with the isotopically separated source, and  $\gamma$ - $\gamma$  coincidence studies with the second source prepared from the enriched sample. The  $\gamma$ -ray singles spectra were recorded with a 35-cm<sup>3</sup> Ge(Li) detector which had a resolution of 2.8 keV and an efficiency of 3.5% relative to a 3-in.  $\times$  3-in. NaI detector at 1.33 MeV. The data were analyzed by computer programs. The intensities of weaker peaks were cross-checked by hand analysis. The room background was carefully measured to eliminate background peaks that appear in the long runs required. Short runs were recorded with internal standards of  $^{57}\text{Co}$ ,  $^{51}\text{Cr}$ ,  $^{56}\text{Co}$ ,  $^{137}\text{Cs}$ , and  $^{208}\text{Tl}$  to obtain the energies of the stronger transitions in the  $^{205}\text{Bi}$  decay. These transitions were in turn used to obtain the energies of the weak transitions in the long runs.

The conversion-electron spectrum was measured with a Si(Li) detector system.<sup>5</sup> The data were analyzed by hand. Lines which were close together were resolved by using the line shape of a nearby singlet.

$\gamma$ - $\gamma$  coincidence measurements were performed with 15- and 35-cm<sup>3</sup> Ge(Li) detectors coupled to a Nuclear Data 3300 two-parameter analyzer with dual 4096-channel analog-to-digital converters. The two germanium detectors were located at 90° and were surrounded by lead cones to minimize crystal-to-crystal Compton scattering. An ORTEC fast-coincidence system with resolving time  $-2\tau = 60$  nsec full width at half maximum, with cross-over timing was used to provide an external gate for the two-dimensional analyzer equipped with a buffer memory and a magnetic tape unit. The total energy range covered in each dimension was

up to 2700 keV.

The data were analyzed with a digital band selector. Gates were set on the photopeak of interest and on the background either just above or below the photopeak to subtract out the Compton background contribution in each gate. The source strength and resolving time were chosen such that chance coincidences were negligible. Linear plots were made of each coincidence spectrum. Relative intensities were obtained from peak-height analysis of these plots. Then for gates that involved possible doublets, or the placement of previously unplaced transitions, numerical printouts were made, and intensities were obtained from summing the net counts in each peak. Over half the gates were analyzed in this latter manner.

The  $\gamma$ -ray singles spectrum was also measured at Livermore with a 7-cm<sup>3</sup> 12-mm-depletion-depth Ge(Li) detector which was the central detector in a Compton suppression spectrometer.<sup>6</sup> The system consists of the germanium detector housing enclosed by two 9-in.-diam by 4.5-in.-thick NaI(Tl) scintillation detectors machined to allow maximum enclosure of the Ge(Li) detector. Typical resolutions obtained with this system are 1.0, 2.0, and 3.0 keV at 122, 1332, and 2754 keV, respectively.

The traditional method of measuring standards and unknowns simultaneously was used to determine the energy of the more prominent  $\gamma$  rays in the  $^{205}\text{Bi}$  decay by using a well-stabilized, well-calibrated singles Ge(Li) detector system.<sup>7</sup> Efficiency determinations were carried out with standards obtained from the International Atomic Energy Agency in Vienna. The sources include  $^{241}\text{Am}$ ,  $^{57}\text{Co}$ ,  $^{203}\text{Hg}$ ,  $^{137}\text{Cs}$ ,  $^{54}\text{Mn}$ ,  $^{60}\text{Co}$ , and  $^{88}\text{Y}$ . The efficiency curve was extended to 2.8 MeV by using  $^{24}\text{Na}$ . Errors adopted for the final efficiency curve are  $\pm 4\%$  from 50 to 200 keV, and  $\pm 2\%$  from 200 keV to 3 MeV.

The relative  $\gamma$ -ray intensities were obtained by using a computer code entitled SAMPO.<sup>6,8</sup> Essentially, the code uses strong singlet peaks in the spectrum of interest to define a set of peak-shape parameters which through interpolation are applicable over the entire spectral region. These shape parameters contain all the information on tailing, energy, and count-rate dependence characteristic of germanium detectors.<sup>8</sup>

### III. RESULTS

Figure 1 shows a Calcomp plot of the Compton-suppressed spectrum of  $^{205}\text{Bi}$  from one of the isotopically separated sources. A single- or double-escape peak is denoted by an upper-case S or D, while a lower-case d indicates the presence of a

doublet, and t, a triplet. One sees from these spectra that there is very little  $^{206}\text{Bi}$  in the source. The results of these  $\gamma$ -ray measurements are given in Table I. There is excellent agreement between the Vanderbilt and Livermore results on both energies and intensities. The adopted values shown in columns 1 and 2 are averages of these two measurements. The intensities of the close doublet transitions were obtained from a quantitative analysis of the coincidence spectra. The results of Rupp and Vegors<sup>4</sup> are listed in column 5. The agreement between our adopted intensity values and those of Rupp and Vegors is very good except above 1600 keV, where their results are systematically about 10% lower than ours on the strong transitions. There is, however, overlap within their error limits of 11%. In addition to the many new transitions seen in our work, several transitions that were only tentatively reported by Rupp and Vegors are confirmed. The 147.32-, 157.27-, and 553.72-keV transitions they reported<sup>4</sup> and a 1128.08-keV transition from an earlier work<sup>9</sup> are definitely not seen in our work. If present, their intensities must be considerably less than reported.<sup>4,9</sup>

40 coincidence gates were analyzed. The coincidence results are given in Table II. The coincidence data were quantitatively analyzed by a hand analysis of the photopeak area in all cases where doublets were suspected or found and in other cases where such information was important in the placement of a transition. Very careful quantitative analysis of the coincidence data must be carried out in such complex decays when such doublets are possible. Figures 2-4 illustrate the quality of these data. In Fig. 3, for example, one sees that the spectrum coincident with the 570.6-keV transition shows no evidence for transition in coincidence with the very close 573.8-keV one. This spectrum illustrates, as well, the clear establishment and placement of one of the weak members of the multiplet around 987 keV. The absence of an entry in Table II indicates that no evidence was found for a peak at that energy above background; while an upper-case N before an entry indicates that a careful quantitative search of the gated data showed this transition was definitely not in coincidence with that gate, e.g., a transition with that singles intensity would have been clearly seen if it were present.

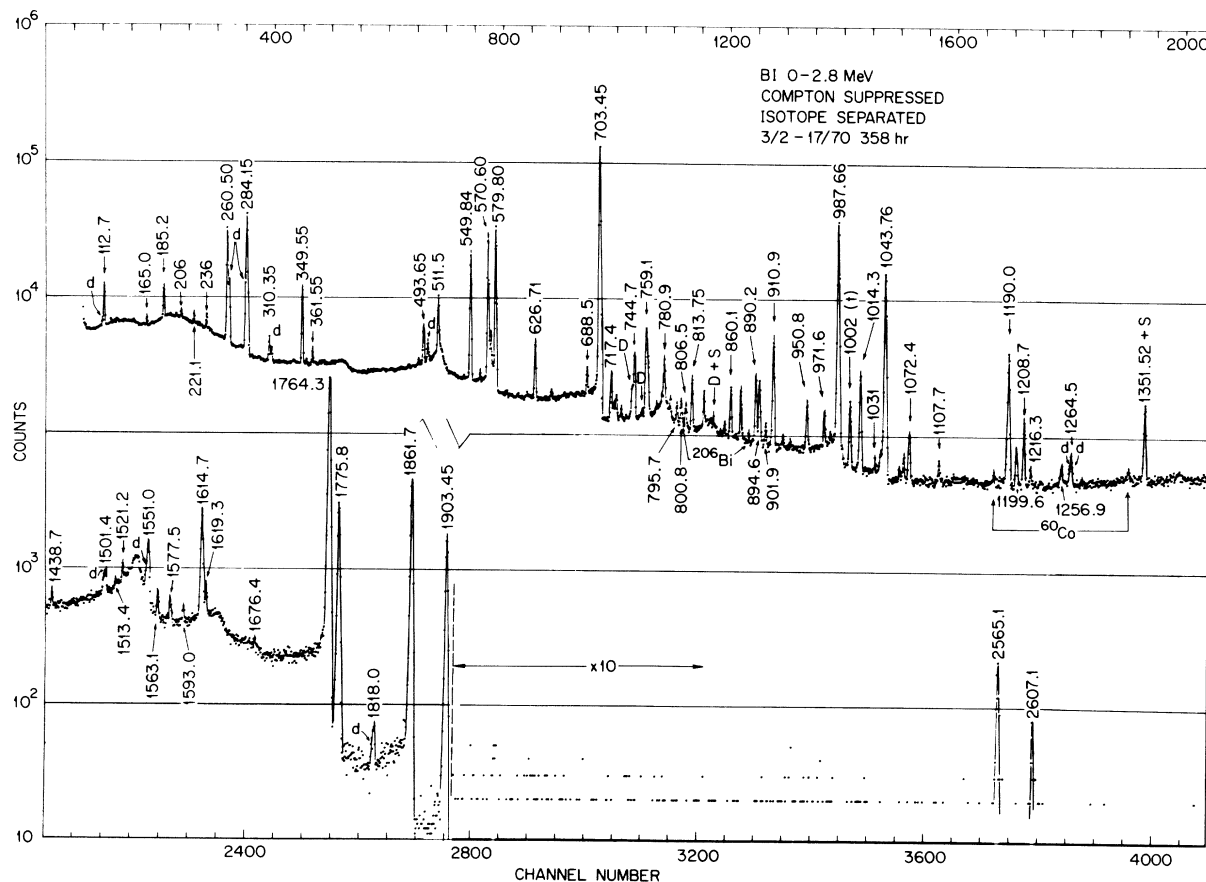


FIG. 1. The  $\gamma$ -ray spectrum of  $^{205}\text{Bi}$  taken with a Compton suppression system and an isotopically separated source.

TABLE I. Energies and intensities of  $\gamma$  rays in  $^{205}\text{Pb}$  from the decay of  $^{205}\text{Bi}$ . The errors in the intensities obtained at Vanderbilt and Livermore were given by the computer programs. The primary difference in the assigned errors of the strong transitions arise from the larger error assigned to the relative-efficiency corrections in the Vanderbilt data. The adopted values are the averages from these two measurements. The most recently published intensities (Ref. 4) are given for comparison.

$E$ (keV)	Adopted values		Vanderbilt	Livermore	Idaho
	$I_\gamma$	$I_\gamma$	$I_\gamma$	$I_\gamma$	$I_\gamma$
2.34 <sup>a</sup>					
26.13 <sup>a</sup>	44 000 ± 4400 <sup>a</sup>				
112.7 ± 0.1 <sup>b</sup>	28 ± 2			28 ± 2	
115.10 ± 0.10	240 ± 10		222 ± 10	254 ± 10	230 ± 40
122.66 ± 0.10 <sup>b</sup>	22 ± 2			22 ± 2	50 ± 10 <sup>c</sup>
127.0 ± 0.2	10 ± 2			10 ± 2	
129.62 ± 0.10	20 ± 2			20 ± 2	30 ± 10 <sup>c</sup>
148.8 ± 0.2 <sup>b</sup>	17 ± 5			17 ± 2	20 ± 10
164.95 ± 0.10	50 ± 3			50 ± 3	50 ± 20 <sup>c</sup>
170.8 ± 0.2	13 ± 3			13 ± 3	
185.22 ± 0.10	305 ± 20		400 ± 25	284 ± 10	280 ± 50
205.74 ± 0.07	81 ± 10		120 ± 10	69 ± 5	100 ± 20
221.07 ± 0.07	100 ± 6		100 ± 6	98 ± 8	90 ± 20
235.97 ± 0.06	182 ± 10		200 ± 10	164 ± 8	170 ± 50
248.4 ± 0.2	6 ± 4			6 ± 4	
259.46 ± 0.20 <sup>d</sup>	160 ± 80	} 3500 ± 100	4000 ± 120	3540 ± 70	3150 ± 470
260.50 ± 0.05	3500 ± 100				
262.80 ± 0.05	1170 ± 40		1270 ± 40	1140 ± 25	1210 ± 210
277.2 ± 0.5	50 ± 10		50 ± 10		
282.38 ± 0.07	1370 ± 20		1380 ± 30	1350 ± 30	1170 ± 120
284.15 ± 0.10	5440 ± 70	} 5590 ± 100	5590 ± 100	5500 ± 100	4880 ± 760
284.26 ± 0.10 <sup>d</sup>	100 ± 30				
310.35 ± 0.05	336 ± 10		356 ± 15	320 ± 10	275 ± 50
312.84 ± 0.20 <sup>d</sup>	80 ± 30		222 ± 8	168 ± 8	180 ± 30
313.43 ± 0.20 <sup>d</sup>	110 ± 30				
339.25 ± 0.20 <sup>b</sup>	35 ± 5		40 ± 10	30 ± 5	
349.55 ± 0.05	1810 ± 30		1850 ± 55	1780 ± 20	1510 ± 170
354.45 ± 0.10	55 ± 6		54 ± 7	56 ± 8	80 ± 10
361.20 ± 0.20 <sup>d</sup>	100 ± 30		200 ± 9	196 ± 8	180 ± 40
361.85 ± 0.20 <sup>d</sup>	98 ± 30				
444.8 ± 0.7	44 ± 20			44 ± 20	
476.30 ± 0.15	75 ± 10		75 ± 12	80 ± 15	
488.05 ± 0.15	125 ± 15		100 ± 25	142 ± 14	190 ± 60 <sup>c</sup>
493.65 ± 0.05	1200 ± 25		1180 ± 36	1220 ± 25	1000 ± 140
498.40 ± 0.15	300 ± 50			305 ± 75	
498.87 ± 0.20 <sup>d</sup>	130 ± 80	} 610 ± 20	610 ± 20	330 ± 75	560 ± 130 <sup>c</sup>
499.54 ± 0.20 <sup>d</sup>	200 ± 50				
503.4 ± 0.5	25 ± 15		25 ± 15		
511.50 ± 0.05	2750 ± 50 <sup>e</sup>		3020 ± 100	2750 ± 40 <sup>e</sup>	3300 ± 350 <sup>f</sup>
549.84 ± 0.04	9490 ± 100		9380 ± 280	9580 ± 100	9030 ± 940
561.27 ± 0.05	170 ± 15		153 ± 15	183 ± 16	200 ± 60 <sup>c</sup>
570.60 ± 0.05	13 940 ± 200		13 680 ± 400	14 180 ± 140	13 450 ± 1540
573.85 ± 0.05	2000 ± 40		2020 ± 60	1970 ± 50	1760 ± 380
576.30 ± 0.10	605 ± 20		610 ± 15	598 ± 40	1110 ± 130
579.80 ± 0.10	17 500 ± 200		17 300 ± 500	17 700 ± 180	17 070 ± 1760
606.25 ± 0.15	80 ± 13			80 ± 13	
626.71 ± 0.10	1880 ± 20		1880 ± 56	1880 ± 20	1810 ± 200
646.00 ± 0.10 <sup>g</sup>	210 ± 10		197 ± 10	220 ± 22	200 ± 40
661.40 ± 0.15	90 ± 15		100 ± 20	80 ± 18	
668.6 ± 0.6 <sup>b</sup>	60 ± 40			60 ± 40	
669.8 ± 1.2 <sup>b</sup>	30 ± 40			30 ± 40	
683.5 ± 0.3 <sup>b</sup>	85 ± 10		90 ± 10	81 ± 26	
688.50 ± 0.05	730 ± 30		700 ± 25	760 ± 30	640 ± 90

TABLE I (Continued)

$E$ (keV)	Adopted values $I_\gamma$	Vanderbilt $I_\gamma$	Livermore $I_\gamma$	Idaho $I_\gamma$
701.16 ± 0.20 <sup>d</sup>	500 ± 200			
703.45 ± 0.05	100 000	101 720	101 720	101 720
704.86 ± 0.20 <sup>d</sup>	1220 ± 300			
717.37 ± 0.05	1000 ± 20	1000 ± 30	990 ± 20	780 ± 170
720.65 ± 0.10	460 ± 30	538 ± 20	378 ± 20	380 ± 100
723.09 ± 0.20 <sup>d</sup>	90 ± 40			
723.57 ± 0.05	490 ± 40	574 ± 20	586 ± 20	540 ± 110
729.40 ± 0.05	210 ± 12	208 ± 12	211 ± 18	260 ± 170
744.70 ± 0.10	2240 ± 50	2500 ± 300 <sup>h</sup>	2240 ± 35	2370 ± 280
757.09 ± 0.20 <sup>d</sup>	400 ± 150			
759.10 ± 0.10	3330 ± 150	3580 ± 120	3820 ± 60	3790 ± 430
761.35 ± 0.10	2200 ± 100	2420 ± 80	2050 ± 40	2210 ± 330
764.99 ± 0.20 <sup>d</sup>	30 ± 12			
771.40 ± 0.15	150 ± 12	147 ± 12	162 ± 30	110 ± 30
777.85 ± 0.15 <sup>b</sup>	235 ± 30	292 ± 35	183 ± 36	
780.92 ± 0.05	1840 ± 30	1860 ± 56	1830 ± 40	1590 ± 320
788.13 ± 0.15	320 ± 50	390 ± 50	300 ± 35	
789.3 ± 0.2	60 ± 30	60 ± 30		370 ± 60
795.67 ± 0.05	450 ± 20	460 ± 15	436 ± 25	440 ± 140
800.80 ± 0.05	610 ± 20	580 ± 20	645 ± 25	430 ± 80 <sup>c</sup>
806.55 ± 0.10	510 ± 40	435 ± 20	588 ± 25	540 ± 160
813.75 ± 0.10	1510 ± 40	1450 ± 50	1550 ± 35	1520 ± 250
828.22 ± 0.05	930 ± 40	990 ± 50	880 ± 30	980 ± 140
831.0 ± 0.3	130 ± 30	130 ± 30		
842.8 ± 0.3	70 ± 20	70 ± 20		
848.2 ± 0.3	85 ± 12		85 ± 12	
852.90 ± 0.05	232 ± 15	232 ± 20	232 ± 20	230 ± 50
860.13 ± 0.05	1400 ± 25	1410 ± 45	1392 ± 25	1420 ± 32
871.95 ± 0.05	1340 ± 30	1320 ± 40	1350 ± 30	1340 ± 190
890.15 ± 0.05	2180 ± 30	2180 ± 65	2180 ± 40	2100 ± 240
894.56 ± 0.05	2000 ± 30	2020 ± 60	1980 ± 40	2750 ± 360
901.90 ± 0.05	415 ± 15	406 ± 15	425 ± 25	430 ± 80
910.90 ± 0.05	5280 ± 100	5410 ± 160	5190 ± 75	5340 ± 580
922.15 ± 0.10	170 ± 10	160 ± 10	185 ± 25	200 ± 40 <sup>c</sup>
931.50 ± 0.15 <sup>b</sup>	125 ± 15	130 ± 15	119 ± 20	180 ± 20
950.84 ± 0.05	1250 ± 30	1258 ± 40	1240 ± 30	1300 ± 150
971.56 ± 0.05	900 ± 20	870 ± 30	926 ± 30	930 ± 190
978.50 ± 0.10	130 ± 20	100 ± 15	166 ± 25	120 ± 30
987.49 ± 0.20 <sup>d</sup>	300 ± 100			
987.66 ± 0.05	51 880 ± 500	52 300 ± 1500	52 300 ± 500	54 260 ± 5550
989.12 ± 0.20 <sup>d</sup>	<100			
989.84 ± 0.20 <sup>d</sup>	240 ± 80		410 ± 50	
992.65 ± 0.20 <sup>d</sup>	280 ± 100			
1001.59 ± 0.20 <sup>d</sup>	820 ± 140			
1001.95 ± 0.20 <sup>d</sup>	880 ± 140	1940 ± 60	1700 ± 100	1820 ± 260
1003.0 ± 0.30	230 ± 100		228 ± 100	
1013.40 ± 0.15 <sup>d</sup>	265 ± 60			
1013.8 ± 0.1 <sup>i</sup>	185 ± 40	3360 ± 100	3410 ± 50	3150 ± 430
1014.30 ± 0.05	2940 ± 60			
1031.5 ± 0.3	110 ± 35		110 ± 35	130 ± 30 <sup>c</sup>
1038.86 ± 0.24	365 ± 30	406 ± 40	324 ± 40	
1043.75 ± 0.05	24 150 ± 300	24 200 ± 700	24 100 ± 250	24 280 ± 2770
1060.75 ± 0.15	142 ± 15	123 ± 10	162 ± 16	
1063.90 ± 0.15 <sup>b</sup>	80 ± 15	98 ± 10	63 ± 20	

TABLE I (Continued)

Adopted values		Vanderbilt	Livermore	Idaho
$E$ (keV)	$I_\gamma$	$I_\gamma$	$I_\gamma$	$I_\gamma$
1066.03 ± 0.15	352 ± 15	327 ± 20	378 ± 18	350 ± 50
1072.40 ± 0.10	972 ± 20	960 ± 30	984 ± 25	1020 ± 160
1075.10 ± 0.10 <sup>b</sup>	35 ± 15		35 ± 15	
1107.72 ± 0.10	318 ± 30	278 ± 18	358 ± 20	380 ± 90
1190.03 ± 0.05	7270 ± 200	7030 ± 200	7450 ± 110	7470 ± 820
1199.62 ± 0.10	610 ± 40	561 ± 25	661 ± 50	640 ± 170
1208.70 ± 0.05	1645 ± 30	1640 ± 50	1645 ± 40	1680 ± 210
1216.25 ± 0.10	324 ± 15	325 ± 15	323 ± 22	230 ± 50 <sup>c</sup>
1256.9 ± 0.5	70 ± 35		70 ± 35	
1261.65 ± 0.20	198 ± 20	183 ± 20	212 ± 30	
1264.60 ± 0.20 <sup>d</sup>	160 ± 70)			
1264.8 ± 0.2	400 ± 70)	586 ± 30	536 ± 50	850 ± 130
1265.9 ± 0.3 <sup>b, f</sup>	150 ± 40	152 ± 40	146 ± 70	
1277.2 ± 0.2 <sup>b</sup>	122 ± 14	132 ± 20	114 ± 20	
1351.52 ± 0.05	3400 ± 100	3580 ± 110	3210 ± 60	3580 ± 530
1438.7 ± 0.2 <sup>b</sup>	375 ± 20	358 ± 25	394 ± 40	350 ± 70 <sup>c</sup>
1499.00 ± 0.15	550 ± 45)		548 ± 45)	
1501.40 ± 0.10	730 ± 45)	1271 ± 40	735 ± 45)	970 ± 360
1513.40 ± 0.20	225 ± 40	200 ± 50	249 ± 50	
1521.20 ± 0.10	640 ± 40	638 ± 25	649 ± 50	650 ± 160
1548.65 ± 0.15	900 ± 50	915 ± 50	868 ± 100	
1551.00 ± 0.10	3120 ± 80	3250 ± 100	2990 ± 100	3400 ± 700
1563.15 ± 0.10	530 ± 30	480 ± 30	580 ± 45	740 ± 160
1577.50 ± 0.15	535 ± 30	525 ± 30	548 ± 45	520 ± 190
1593.00 ± 0.15	370 ± 25	356 ± 25	386 ± 40	340 ± 160
1614.30 ± 0.15	7320 ± 120	7400 ± 220	7280 ± 115	6470 ± 780
1619.10 ± 0.15	1180 ± 50	1280 ± 40	1080 ± 55	770 ± 100
1676.4 ± 0.3	105 ± 20	102 ± 20	109 ± 30	
1756.4 ± 0.3	700 ± 40	710 ± 40	690 ± 75	
1760.04 ± 0.40 <sup>d</sup>	400 ± 100			
1764.30 ± 0.10	104 400 ± 2000	100 600 ± 3000	107 300 ± 1100	94 630 ± 10 290
1775.80 ± 0.10	12 820 ± 250	12 570 ± 372	13 080 ± 220	11 280 ± 1330
1815.6 ± 0.4	44 ± 15		44 ± 15	
1818.0 ± 0.2 <sup>j</sup>	152 ± 12	174 ± 12	152 ± 18	170 ± 40
1861.70 ± 0.10	19 840 ± 300	19 400 ± 550	20 200 ± 250	17 750 ± 1980
1903.45 ± 0.10	7930 ± 120	7800 ± 230	8040 ± 120	6820 ± 760
1965.8 ± 0.5	26 ± 5	27 ± 7	25 ± 6	50 ± 20
2003.3 ± 0.5 <sup>b</sup>	12 ± 5	8 ± 4	16 ± 5	
2565.10 ± 0.15	136 ± 7	140 ± 7	132 ± 8	160 ± 60
2607.1 ± 0.20	60 ± 6	94 ± 8	58 ± 6	70 ± 20

<sup>a</sup> Conversion-electron measurement. The total intensity of the 26.1-keV transition, as given in the table, was obtained from our coincidence work (see text).

<sup>b</sup> Not placed in the decay scheme.

<sup>c</sup> Transition was seen only once by Rupp and Vegors (Ref. 4).

<sup>d</sup> Energy deduced from energy levels in decay scheme. Transition based on coincidence data from which the  $\gamma$  intensity, given in column 2, was obtained.

<sup>e</sup> Essentially free of annihilation radiation.

<sup>f</sup> This transition is only tentatively assigned to the <sup>205</sup>Bi decay.

<sup>g</sup> Coincidence data indicated that less than one half of the 646.00-keV transition should be placed as shown in the present level scheme. However, the coincidence statistics of this transition are rather poor.

<sup>h</sup> The analysis of the intensity of this line is complicated by the presence of the double-escape peak of the 1764.30-keV transition. This double-escape peak at 742.3 keV is stronger than the 744.70-keV photopeak.

<sup>i</sup> Energy obtained from conversion-electron measurements. Intensity obtained from conversion coefficients, conversion-electron intensities, and total  $\gamma$ -ray intensities.

<sup>j</sup> Possible doublet.

TABLE II. Coincidence results from two-parameter  $\gamma$ - $\gamma$  experiments in the decay of  $^{205}\text{Bi}$ . A qualitative indication of the relative strengths of the  $\gamma$  rays appearing in each coincidence gate is shown by: Strongest lines are underlined, e.g., 703.5; medium strength lines are written normally, e.g., 703.5; and weak lines are underlined partially, e.g., 703.5. The absence of an energy indicated that no peak was observed above background at that energy in the gate. Transitions where a quantitative analysis of the data indicated that the transition, if in coincidence, should have been seen above the background, but was not observed, are identified by N, e.g., N-646.0.

Gated $E_\gamma$ (keV)	$\gamma$ -rays observed in coincidence gate
259.5) 260.5 } 262.8)	<u>312.8-313.4</u> , <u>349.6</u> , 498.4-498.9-499.5, 511.5, <u>549.8</u> , <u>570.6</u> , N-646.0, <u>701.1</u> , 780.9, N-828.2, <u>950.8</u> , <u>1001.6-1002.0</u> , <u>1208.7</u> , <u>1351.5</u> , N-1438.7, 1499.0, 1501.4, 1513.4, N-1551.0, N-1593.0, N-1756.4
282.4) 284.2)	549.8, <u>570.6</u> , <u>703.5</u> , <u>759.1</u> , <u>761.4</u> , N-828.2, <u>1208.7</u> , N-1438.7, N-1551.0, N-1593.0, 1619.1
349.6	<u>260.5</u> , <u>262.8</u> , 561.3, <u>573.9</u> , <u>576.3</u> , <u>688.5</u> , 703.5, <u>1001.6-1002.0</u> , 1261.7, 1264.6-1264.8
493.7	236.0, <u>312.8-313.4</u> , <u>493.7</u> , <u>744.7</u>
511.5	115.1, <u>259.5</u> , 284.2, 703.5, 704.9, N-828.2, <u>987.5-987.7</u> , <u>1066.0</u> , <u>1107.7</u>
549.8	260.5, 262.8, <u>282.4</u> , 759.1, 761.4, 780.9, 894.6, 971.6, <u>1043.8</u>
561.3	703.5
570.6	<u>260.5</u> , <u>262.8</u> , <u>282.4</u> , 759.1, 761.4, 780.9, 950.8, 992.7, <u>1043.8</u>
573.9) 576.3)	<u>185.2</u> , <u>282.4</u> , <u>349.6</u> , N-646.0, 688.5, N-828.2, 1199.6, N-1438.7, N-1551.0, N-1593.0, N-1756.4
579.8	<u>894.6</u> , <u>971.6</u> , 1013.4
626.7	703.5, <u>987.5-987.7</u>
688.5	<u>349.6</u> , 498.4-498.9-499.5, <u>573.9</u> , <u>576.3</u>
703.5	<u>284.2</u> , <u>310.4</u> , <u>312.8-313.4</u> , <u>511.5</u> , 570.6, 626.7, N-646.0, 795.7, N-828.2, 860.1, <u>872.0</u> , <u>890.2</u> , <u>910.9</u> , 950.8, <u>971.6</u> , <u>987.5-987.7</u> , <u>1001.6-1002.0</u> , <u>1072.4</u> , 1351.5, N-1438.7, 1548.7, N-1551.0, N-1593.0, N-1756.4, <u>1861.7</u> , <u>1903.5</u>
744.7	<u>493.7</u> , 729.4, 806.6
759.1) 761.4)	<u>282.4</u> , 549.8, 570.6, N-646.0, 703.5, 800.8, <u>813.8</u> , N-828.2, 852.9, 987.5-987.7, 1003.0, <u>1014.3</u> , 1208.7, N-1438.7, N-1551.0, N-1593.0, N-1756.4, 1760.0
780.9	<u>260.5</u> , <u>262.8</u> , <u>549.8</u> , <u>570.6</u>
813.8	573.9, 576.3, <u>759.1</u> , <u>761.4</u> , 989.8, <u>1031.5</u>
828.2	361.2-361.9, <u>723.1-723.6</u>
860.1	<u>282.4-284.2</u> , <u>703.5</u> , <u>717.4</u> , <u>987.5-987.7</u> , <u>1001.6-1002.0</u>
872.0	<u>703.5</u> , 989.8
890.2	<u>703.5</u> , 894.6
910.9	<u>703.5</u> , 950.8, 992.7
950.8	<u>260.5</u> , <u>262.8</u> , 282.4, 349.6, <u>570.6</u> , 703.5, 910.9, <u>1043.8</u> , 1351.5, 1614.3
971.6	<u>549.8</u> , <u>579.8</u> , <u>1043.8</u>
987.5) 987.7 } 989.8 ) 992.7)	115.1, <u>260.5-262.8</u> , <u>511.5</u> , <u>570.6</u> , <u>626.7</u> , N-646.0, 704.9, <u>717.4</u> , 723.1-723.6, 759.1, 761.4, 788.1, 813.8, N-828.2, <u>860.1</u> , 872.0, <u>901.9</u> , 1043.8, <u>1066.0</u> , <u>1107.7</u> , 1216.3, <u>1264.6-1264.8</u> , N-1438.7, N-1551.0, 1577.5, N-1593.0, <u>1619.1</u> , N-1756.4
1001.6) 1002.0)	<u>260.5</u> , <u>262.8</u> , <u>349.6</u> , 701.2, <u>703.5</u> , 759.1, 761.4, <u>860.1</u> , 901.9, <u>987.5-987.7</u>
1013.4) 1014.3)	185.2, 262.8, 498.4-498.9-499.5, 573.9, 579.8, <u>759.1</u> , <u>761.4</u>
1043.8	<u>221.1</u> , <u>349.6</u> , <u>549.8</u> , <u>570.6</u> , N-646.0, 720.7, N-828.2, 894.6, <u>922.2</u> , 950.8, 992.7, <u>1208.7</u> , N-1438.7, <u>1521.2</u> , N-1551.0, <u>1563.2</u> , N-1593.0, N-1756.4

TABLE II (Continued)

Gated $E_\gamma$ (keV)	$\gamma$ -rays observed in coincidence gate
1190.0	284.2, 361.2-361.9
1208.7	260.5, 262.8, 282.4, <u>312.8-313.4</u> , 780.9, <u>1043.8</u>
1264.6 } 1264.8 }	<u>349.6</u> , <u>703.5</u> , 987.5-987.7
1351.5	<u>260.5</u> , <u>262.8</u> , <u>703.5</u>
1499.0 } 1501.4 }	<u>260.5</u> , 262.8
1548.7 } 1551.0 }	<u>703.5</u>
1614.3	N-828.2, 950.8, <u>992.7</u>
1619.1	987.5-987.7
1764.3	<u>488.1</u> , 723.1-723.6, 757.1, 800.8
1775.8	a
1861.7	<u>703.5</u>
1903.5	<u>703.5</u>

<sup>a</sup> No transitions definitely seen.

Most of the possible multiple placements of transitions noted by Rupp and Vegors<sup>4</sup> in their table are now confirmed by our coincidence data. There are a few remaining questionable cases, however. While there is very weak coincidence evidence for a 493.7-keV transition out of the 1758.50-keV level, it would be  $M2$  or of higher multipolarity; hence it probably does not exist. An alternate interpretation of the coincidence data is that there is a 492-keV transition with an intensity of about 20% of the 493.7-keV transition, and it depopulates the 1756.4-keV state. The coincidence data indicate less than  $\frac{1}{4}$  of the 310.35-keV singles intensity can depopulate the 1575.26-keV level, and less than  $\frac{1}{2}$  the 561.27-keV intensity can depopulate this same level. The 561.27-keV transition would be  $M2$  or  $E3$  and so is very unlikely. Thus, these alternate placements for the 310.35- and 561.27-keV transitions are not given in the decay scheme. The 1501-keV transition which depopulates the 1764.31-keV level has two other possible placements out of the 2203.90-keV level and/or out of the 2488.16-keV level. Coincidence data (Fig. 2) show that less than 20% of the 1501.40-keV transition single intensity can go elsewhere in the level scheme. Also it would be an  $M2$  transition out of the 2203.90-keV level.

Table III lists the results of our conversion-electron measurements along with the results of previous investigators.<sup>10-13</sup> Our  $\gamma$ -ray intensities from Table I along with an essentially pure  $E2$  conver-

sion coefficient<sup>10,11</sup> measured for the 703.45-keV transition were used to obtain the conversion coefficients. With our more accurate  $\gamma$  ray and in some cases electron intensities, we have obtained more accurate conversion coefficients. The theoretical conversion coefficients of Hager and Seltzer<sup>14</sup> and Sliv and Band<sup>15</sup> were used to determine the multipolarities. In several cases our assignments are more restrictive than those of Rupp and Vegors<sup>4</sup> because of our better error limits. Table IV lists the results of our  $K/L$  ratio measurements which give added confirmation to several assignments.

#### IV. LEVEL SCHEME

The above data were incorporated into the level scheme shown in Fig. 5. This scheme includes two new levels, positive identification of four of the tentative (dashed) levels reported by Rupp and Vegors,<sup>4</sup> and the nonexistence of a fifth level tentatively suggested by them. In addition, numerous new transitions which include new doublets, triplets, and even a quadruplet are placed. Only careful quantitative analysis of coincidence data obtained with two large Ge(Li) detectors could yield such details. Of the 146 transitions observed in our work, 130 are placed in the level scheme, in most cases on the basis of coincidence data. The coincidence placement of a transition is shown by a solid circle at the depopulating level. The per-

TABLE III.  $K$  conversion coefficients of transitions in  $^{205}\text{Pb}$  and multipolarity assignments based on these data. Below 1600 keV the theoretical conversion coefficients are those of Hager and Seltzer (Ref. 14), and above that, of Sliv and Band (Ref. 15). Units are given as  $\alpha_K \times 10^2$ ; for example,  $\alpha_K$  for the 703.45-keV transition is 0.0110.

$E_\gamma$ (keV)	$I_\gamma$	Refs.	$K$ -electron intensity, $I_{eK}$	Average	Experimental $\alpha_K \times 10^2$	Theoretical $\alpha_K \times 10^2$	Multipole assignment
			Vanderbilt			$E1$ $E2$ $E3$	$M1$
165.22	305	40 ± 4	42 ± 4	41 ± 3	148 ± 21	7.70 20.3 51.6	138
205.74	81	6.6 ± 2.0	6.6 ± 2.0	6.6 ± 2.0	90 ± 20	5.95 15.9 41.9	103
221.07	100	5 ± 2	9.6 ± 2.0	8.0 ± 2.0	88 ± 24	5.00 13.5 35.9	84.2
235.97	182	8 ± 1	15.3 ± 2.0	12.0 ± 2.0	73 ± 15	4.28 11.6 31.1	70.2
260.50	3500	165 ± 15	155 ± 8	160 ± 8	50 ± 6	3.38 4.15 24.7	53.4
282.80	1170	46 ± 5	50 ± 5	48 ± 5	45 ± 7	3.31 8.96 24.2	52.1
282.38	1370	46 ± 5	236 ± 8	48 ± 6	38.5 ± 6.0	2.80 7.56 20.4	42.8
284.15	5440	175 ± 21	175 ± 21	180 ± 20	37 ± 5	2.76 7.45 20.1	42.1
310.35	336	4.3 ± 1.0	10 ± 2	4.3 ± 1.0	14.0 ± 3.0	2.25 6.06 16.3	33.1
312.84	80	4.9 ± 1.0	4.9 ± 1.0	4.9 ± 1.0	28.4 ± 6.5	2.21 5.95 16.0	32.4
313.43	110	4.9 ± 1.0	4.9 ± 1.0	4.9 ± 1.0	28.4 ± 6.5	2.20 5.92 15.9	32.2
349.55	1810	29 ± 2	32 ± 3	30 ± 3	18.2 ± 2.5	1.72 4.60 12.3	24.0
493.65	1200	11 ± 1	9.0 ± 2.0	10 ± 1	9.2 ± 1.3	0.814 2.15 5.42	9.56
498.40	300	4.9 ± 1.5	4.9 ± 1.5	4.9 ± 1.5	8.6 ± 2.8	0.798 2.10 5.31	9.32
498.87	130	4.9 ± 1.5	4.9 ± 1.5	4.9 ± 1.5	8.6 ± 2.8	0.796 2.10 5.29	9.30
499.54	200	4.9 ± 1.5	4.9 ± 1.5	4.9 ± 1.5	8.6 ± 2.8	0.794 2.09 5.28	9.27
511.50	2750	22 ± 3	19 ± 2	20.5 ± 2.0	8.2 ± 1.1	0.756 1.99 5.00	8.70
549.84	9490	6.3 ± 1.6	7.5 ± 1.5	6.9 ± 1.0	0.80 ± 0.14	0.652 1.71 4.24	7.19
570.60	13940	82 ± 8	79 ± 4	80 ± 4	6.35 ± 0.7	0.605 1.58 3.89	6.53
579.80	17500	24 ± 2	24 ± 2	24 ± 1.5	1.51 ± 0.18	0.586 1.53 3.75	6.26
626.71	1880	6.7 ± 1.0	8.0 ± 1.0	7.4 ± 0.7	4.33 ± 0.60	0.502 1.31 3.15	5.11
688.50	730	1.0 ± 0.3	2 ± 1	1.4 ± 0.3	2.11 ± 0.53	0.418 1.09 2.56	4.00
703.45	100000	100	100	100	1.10 ± 0.10 <sup>b</sup>	0.401 1.04 2.44	3.79
717.37	1000	2.0 ± 0.5	3.0 ± 1.0	2.4 ± 0.5	2.64 ± 0.66	0.386 1.00 2.34	3.60
720.65	460	1.5 ± 0.4	1.5 ± 0.4	1.5 ± 0.4	3.59 ± 1.1	0.383 0.995 2.31	3.56
723.57	490	≤ 1.7	≤ 1.7	≤ 1.7	≤ 3.8	0.380 0.988 2.29	3.52
729.40	210	≤ 1.5	≤ 1.5	≤ 1.5	≤ 7.8	0.374 0.972 2.25	3.45
744.70	2240	2.1 ± 0.5	2 ± 1	2.1 ± 0.5	1.03 ± 0.27	0.360 0.934 2.15	3.27
759.10	3300	3.1 ± 0.6	5.0 ± 0.6	3.1 ± 0.6	1.06 ± 0.22	0.347 0.900 2.07	3.11
761.35	2200	2.0 ± 0.5	5.0 ± 0.6	2.0 ± 0.5	1.00 ± 0.22	0.345 0.896 2.06	3.09
813.75	1510	1.1 ± 0.4	1.1 ± 0.4	1.1 ± 0.4	0.81 ± 0.30	0.304 0.788 1.78	2.60
890.15	2180	≤ 0.7	≤ 0.7	≤ 0.7	≤ 0.37	0.258 0.665 1.47	2.06
894.56	2000	9.1 ± 1.0	3.4 ± 0.4	3.4 ± 0.4	1.87 ± 0.30	0.255 0.659 1.46	2.04
910.90	5280	27 ± 2	9.0 ± 1.0	9.0 ± 1.0	1.87 ± 0.28	0.247 0.637 1.40	1.94
987.66	51880	2.1 ± 0.5	26 ± 3	26 ± 2	0.55 ± 0.07	0.213 0.547 1.18	1.58
1001.59	820	1.8 ± 0.4	1.8 ± 0.4	1.9 ± 0.4	1.08 ± 0.22	0.208 0.538 1.15	1.52
1001.95	880	1.8 ± 0.4	1.8 ± 0.4	1.9 ± 0.4	1.08 ± 0.22	0.208 0.533 1.15	1.52
1003.0	230	2.1 ± 0.3	6.5 ± 1.0	2.1 ± 0.3	...	0.207 0.532 1.15	1.52
1013.4	265	2.1 ± 0.3	6.5 ± 1.0	2.1 ± 0.3	...	0.203 0.521 1.12	1.48
1013.8	...	2.1 ± 0.3	6.5 ± 1.0	2.1 ± 0.3	...	0.203 0.521 1.12	1.48
1014.30	2940	3.3 ± 0.4	3.3 ± 0.4	3.3 ± 0.4	1.24 ± 0.20	0.203 0.521 1.12	1.48

TABLE III (Continued)

$E_\gamma$ (keV)	$I_\gamma$	Refs.	K-electron intensity, $I_{ex}$		Average	Experimental $\alpha_K \times 10^2$			Theoretical $\alpha_K \times 10^2$			Multipole assignment
			10-12	Vanderbilt		Vanderbilt	Average	E1	E2	E3	M1	
1043.75	24150	30 ± 2	27 ± 3	28.5 ± 2.0	1.30 ± 0.14	0.193	0.494	1.06	1.37	M1		
1072.40	972	1.2 ± 0.3	1.2 ± 0.3	1.2 ± 0.3	1.30 ± 0.3	0.184	0.470	0.999	1.28	M1, E3 <sup>a</sup>		
1190.03	7270	7.6 ± 1.0	4.8 ± 1.0	6.2 ± 1.0	0.94 ± 0.18	0.154	0.388	0.809	0.984	M1, E3 <sup>a</sup>		
1351.52	3400	1.1 ± 0.3	0.7 ± 0.4	0.95 ± 0.25	0.31 ± 0.09	0.124	0.307	0.627	0.715	E2		
1499.00	550	0.4 ± 0.1	0.4 ± 0.1	0.4 ± 0.1	0.34 ± 0.08	0.103	0.254	0.508	0.549	(E1 <sup>3</sup> , E2)		
1501.40	730	0.8 ± 0.2	0.8 ± 0.2	0.8 ± 0.2	0.28 ± 0.008	0.103	0.254	0.508	0.549	(M1)		
1551.00	3120	3.1 ± 0.6	3.1 ± 0.6	3.1 ± 0.6	0.47 ± 0.11	0.098	0.239	0.476	0.505	E2		
1614.30	7320	40 ± 2	40 ± 2	40 ± 2	0.42 ± 0.05	0.093	0.22	0.44	0.44	M1, E3 <sup>a</sup>		
1764.30	104400	4.6 ± 1.0	1.6 ± 0.4	4.6 ± 1.0	0.39 ± 0.10	0.080	0.18	0.36	0.34	M1, E3 <sup>a</sup>		
1775.80	12820	1.6 ± 0.4	1.6 ± 0.4	1.6 ± 0.4	0.089 ± 0.03	0.080	0.18	0.36	0.36	M1, E3 <sup>a</sup>		
1861.70	19840	0.5 ± 0.1	0.5 ± 0.1	0.5 ± 0.1	0.07 ± 0.02	0.074	0.17	0.33	0.30	E1		
1903.45	7930	0.029 ± 0.005	0.029 ± 0.005	0.029 ± 0.005	0.23 ± 0.06	0.071	0.16	0.31	0.29	E1		
2565.10	136	0.016 ± 0.004	0.016 ± 0.004	0.016 ± 0.004	0.29 ± 0.08	0.33 <sup>c</sup>	0.098	0.18	0.14	M2		
2607.1	60	0.016 ± 0.004	0.016 ± 0.004	0.016 ± 0.004	0.29 ± 0.08	0.32 <sup>c</sup>	0.094	0.17	0.13	M2		

<sup>a</sup> Excluded by known spins and parities.

<sup>b</sup> Experimental value used for normalization (Ref. 11).

<sup>c</sup> M2 theoretical value.

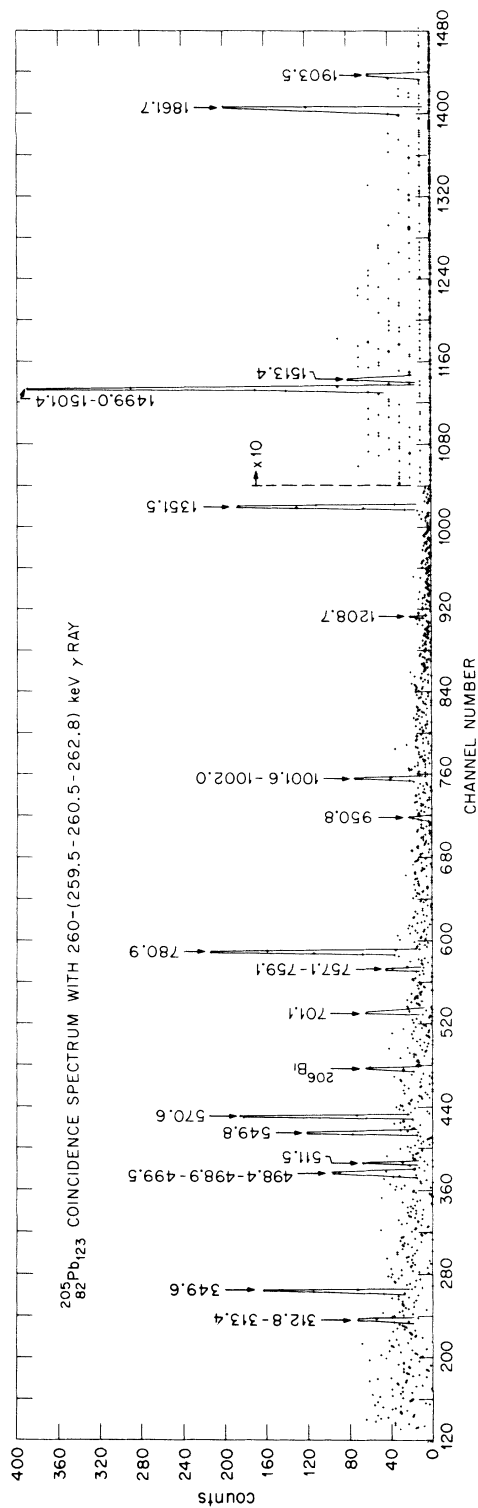


FIG. 2. Coincidence spectrum obtained with the gate set on the 260-keV  $\gamma$  ray. The gate contains the 259.5-, 260.5-, and 262.8-keV  $\gamma$  rays. The spectrum is corrected for Compton background coincidences, but the subtraction is not exact as seen by the presence of the 1861.7- and 1903.5-keV transitions from the Compton coincidences of the 703.44-keV transition.

centage of electron-capture and positron level feedings and  $\log ft$  values for each level are given in Table V. The electron-capture feeding to the 987.66-keV level was obtained from a comparison of the  $K\alpha$  and  $K\beta$  x rays coincident with the 987.66- and 1043.75-keV transitions. The 1043.75-keV level is fed essentially by transitions from higher states. The data were corrected for internal-conversion processes. This procedure was cross-checked by comparison of the  $K$  x rays seen in other gates. Our value of 72% population for the 987.66-keV level by the 26.1-keV transition is in excellent agreement with the value of 70% obtained by internal-conversion measurements.<sup>13</sup>

Since many of the features of the level scheme have been recently discussed by Rupp and Vegors,<sup>4</sup> we have restricted our discussion to the new information gained in our work. While we have added some new transitions to the levels up to 1500 keV, the general features of the levels are unchanged. However, we do not see the 553.72- and 1128.08-keV transitions out of a tentative level suggested<sup>4,9</sup> at 1129.9 keV and so conclude that this level does not exist. Also we see a 1013.40-keV  $E1$  transition from a level at 2607.00 keV in addition to the 1013.8-keV isomeric  $M4$  transition from the 1013.79-keV level.

The latest *Nuclear Data Sheets*<sup>16</sup> give the spin of the 1264.77-keV level as either  $\frac{5}{2}^-$  or  $\frac{7}{2}^-$ . Based on  $\gamma$  transitions to  $\frac{1}{2}^-$ ,  $\frac{3}{2}^-$ ,  $\frac{5}{2}^-$ , and  $\frac{7}{2}^-$  levels and  $\gamma$ -ray feeding from a  $\frac{7}{2}^+$  (or  $\frac{9}{2}^+$ ) level the spin and parity are  $\frac{5}{2}^-$ . Conversion coefficients of  $\frac{7}{2}$  or  $\frac{1}{2}$  for the spin of the 1499.04-keV level are excluded on the basis of a transition to this level from the  $\frac{11}{2}^+$ , 2203.90-keV level, the decay to the ground state, the  $M1$  character of the 511.50-keV transition to a  $\frac{5}{2}^-$  level, and the  $\alpha_K$  of the 745.67-keV transition. Though not given

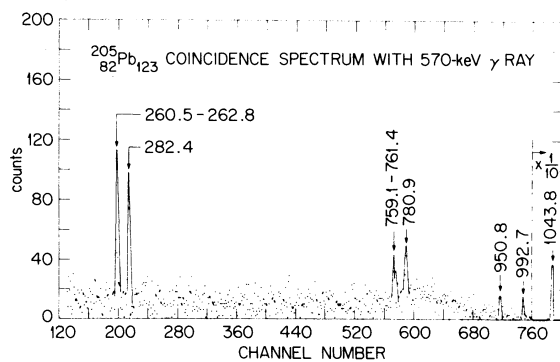


FIG. 3. Coincidence spectrum obtained with the gate on the 570-keV  $\gamma$  ray. The spectrum is corrected for Compton background coincidences.

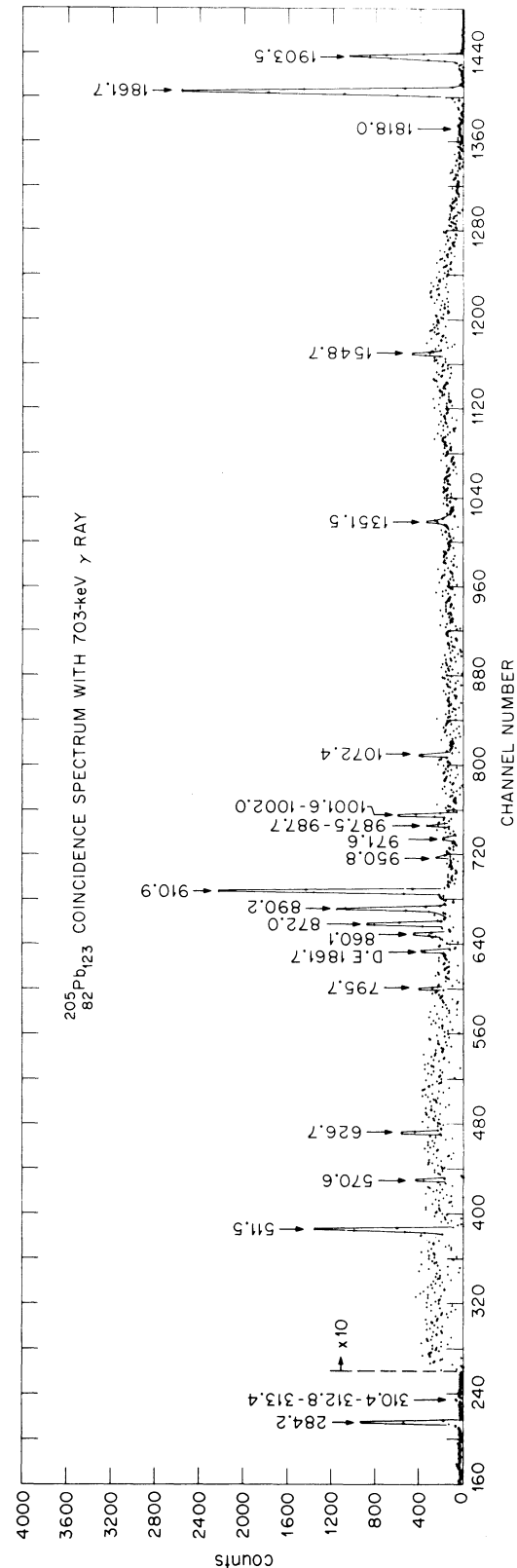


FIG. 4. Coincidence spectrum obtained with the gate on the 703-keV  $\gamma$  ray. The spectrum is corrected for Compton background coincidences.

in Table III this  $\alpha_K$  is definitely not  $M2$ , as a  $\frac{11}{2}^+$  assignment would require.

The 1575.26-keV level was only tentatively reported earlier.<sup>4</sup> The data from the 813.8- and 872.0-keV gates, as well as other gates, definitely establish this level. Odd parity is established by the  $\alpha_K$  value of the 871.95-keV transition to a  $\frac{7}{2}^-$  level. Based on the decay to  $\frac{7}{2}^-$  and  $\frac{5}{2}^-$  levels and population from  $\frac{9}{2}^+$  levels, the spin and parity is  $\frac{9}{2}^-$  or  $\frac{7}{2}^-$ .

The 1705.03-keV level is definitely established by the 860-, 987-, and 1002-keV gates. The  $\alpha_K$  of the 717.4-keV transition to a  $\frac{9}{2}^-$  level is used to establish odd parity for the level. This level definitely decays to  $\frac{7}{2}^-$  and  $\frac{9}{2}^-$  levels and is fed by transitions from  $\frac{9}{2}^+$  and  $\frac{11}{2}^+$ . These transitions coupled with the odd parity indicate a spin and parity of  $\frac{11}{2}^-$  or  $\frac{9}{2}^-$ .

The 1756.4-keV level is new. It is based solely on the fact that we searched carefully every gate that involved transitions from levels up to 1.1 MeV and definitely concluded that the 1756.4-keV transition does not populate any excited state below that energy. With a decay energy of  $2703 \pm 6$  keV,<sup>17</sup> this transition must feed the ground state or the 2.34-keV level. While the energy fits the gap 1758.50 to 2.34 keV, these levels are  $\frac{9}{2}^+$  (or  $\frac{11}{2}^+$ ) and  $\frac{1}{2}^-$ , respectively, and such a transition would not be seen with the intensity observed for the 1756.4-keV transition. While no other transitions are definitely established to populate or depopulate this level, there are several cases where relatively weak transitions could have been masked, such as 491.6- and 742.6-keV transitions out of and the 495.7- and 808.6-keV transitions into the level.

Based on transitions into the 1758.50-keV level from  $\frac{7}{2}^+$ ,  $\frac{9}{2}^+$ , and  $\frac{11}{2}^+$  levels and transitions out to  $\frac{9}{2}^-$  and  $\frac{13}{2}^+$  levels, the spin and parity assignment suggested for the 1758.50-keV level is  $\frac{9}{2}^+$ . This is supported by the  $E2$  character of the 744.70-keV transition from the  $\frac{7}{2}^+$  state.

TABLE IV.  $K/L$  ratios of transitions in <sup>205</sup>Pb.

$E_\gamma$ (keV)	$K/L$ ratios			
	Experimental	Theoretical		
		$E1$	$E2$	$M1$
260.50	5.5 ± 0.7	6.0	1.4	5.6
262.80	5.8 ± 0.7	6.0	1.4	5.6
349.55	4.9 ± 1.3	6.2	2.2	5.6
570.60	5.8 ± 1.2	6.3	3.4	5.6
579.80	3.5 ± 0.8	6.3	3.5	5.6
703.45	4.6 ± 0.4	6.4	4.2	5.6
987.66	5.6 ± 0.8	6.5	4.9	5.7
1043.75	6.8 ± 1.0	6.5	4.9	5.7
1764.30	6.6 ± 0.8	6.7	5.2	5.7

A level at 1818 keV is tentatively proposed on the basis of the 1818.0- and 1815.6-keV transitions which are separated by the energy of the first excited state. A strong coincidence relation was observed between the 1818.0- and 703.45-keV transitions by Rupp and Vegors.<sup>4</sup> However, the 1818.0-

TABLE V. The electron-capture level feedings in <sup>205</sup>Bi decay and  $\log ft$  values. The total decay energy is 2703 keV.

Level energy (keV)	Spin and parity of levels	$\beta^+$ and/or electron capture <sup>a</sup>	$\log ft$
2.34	$\frac{1}{2}^-$	0	...
262.82	$\frac{3}{2}^-$	0 ± 0.07	...
576.25	$\frac{3}{2}^-$	0.05 ± 0.04	...
703.44	$\frac{7}{2}^-$	14.5 ± 0.102	9.1
761.36	$\frac{5}{2}^-$	-0.14 ± 0.08	...
987.66	$\frac{9}{2}^-$	14.1 ± 0.15	9.0
1013.79	$\frac{13}{2}^+$	3.56 ± 0.10	9.6
1043.75	$\frac{7}{2}^-$	0.03 ± 0.09	...
1264.77	$\frac{5}{2}^-$	-0.11 ± 0.08	...
1499.04	$\frac{9}{2}^-$	0.004 ± 0.02	...
1575.26	$\frac{9}{2}^-, \frac{7}{2}^-$	0.68 ± 0.03	9.9
1593.59	$\frac{9}{2}^+$	7.2 ± 0.064	8.8
1614.35	$\frac{7}{2}^-$	9.9 ± 0.08	8.7
1705.03	$\frac{11}{2}^-, \frac{9}{2}^-$	0.02 ± 0.04	...
1756.4	...	0.19 ± 0.01	10.3
1758.50	$\frac{9}{2}^+$	0.13 ± 0.02	10.4
1764.31	$\frac{7}{2}^-$	28.6 ± 0.55	8.1
1775.79	$\frac{7}{2}^-$	4.8 ± 0.07	8.9
1818 <sup>b</sup>	$\frac{5}{2}^-$	≤ 0.01	...
1842.01	( $\frac{13}{2}^+$ )	0.14 ± 0.017	10.3
1965.9	$\frac{9}{2}^-, \frac{7}{2}^-$	0.23 ± 0.055	10.0
2203.90	$\frac{11}{2}^+$	2.43 ± 0.098	8.5
2252.26	$\frac{7}{2}^+$	1.13 ± 0.05	8.8
2488.16	$\frac{9}{2}^+, \frac{7}{2}^+$	0.94 ± 0.01	8.0
2521.40	$\frac{9}{2}^-, \frac{7}{2}^-$	0.28 ± 0.03	8.3
2565.10	$\frac{9}{2}^+$	8.16 ± 0.09	6.5
2607.00	$\frac{9}{2}^+$	2.32 ± 0.05	6.3

<sup>a</sup> The feeding is essentially electron capture. For example, the ratio of positron feeding to the electron-capture feeding to the 703.44-keV level is 0.007. The feedings which are essentially zero such as the one to the 576.25-, 761.36-, 1043.75-, 1264.77-, and 1705.03-keV levels are not used for normalization. The negative feeding indicates that there is more intensity going into the level than there is going out.

<sup>b</sup> Only tentatively assigned.

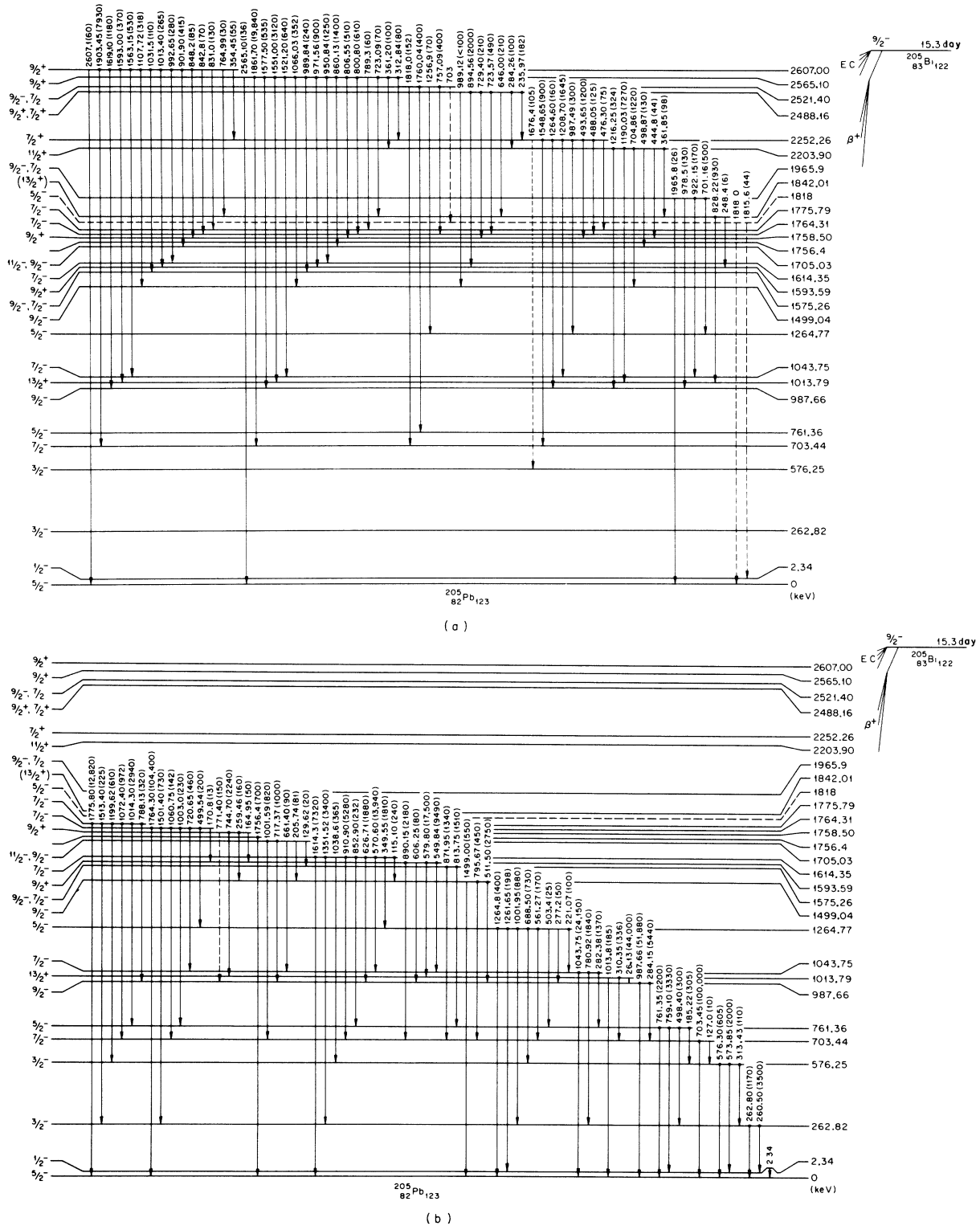


FIG. 5. (a) The level scheme of  $^{205}\text{Pb}$ . Transitions which depopulate the levels from 1818 to 2607 keV are shown. A dot indicates placement on the basis of coincidence data. (b) The level scheme of  $^{205}\text{Pb}$ . Transitions which depopulate the levels up to 1775.79 keV are shown. A dot at the beginning of an arrow indicates the transition was placed by coincidence data.

keV transition is about 7 times stronger than would be expected from its singles intensity. Our data are consistent with the 1818.0-keV transition with our singles intensity (Fig. 4) being in coincidence with the 703.45-keV transition, but the statistics are not sufficient to definitely establish such. Such a coincidence relation is assumed, since the 1818.0-keV transition fits between the known 703.45- and 2521.40-keV levels. However, this could also be satisfied by a 703-keV transition on top of the 1818.0-keV level, or the 1818.0-keV transition could be a doublet and both placements exist. In any case, the 1815.6-keV transition must depopulate a previously unreported level, and an 1818.0-keV level is one such possibility. Since this level is based on the placement of a transition into the 2.34-keV level, the spin and parity of this level would be  $\frac{5}{2}^-$ .

The 1842.0-keV level is based on the 828.2-keV coincidence spectrum and the absence of the 828.2-keV transition in any other gate. A careful search was made for this transition in each gate, which corresponds to the primary transition out of each level. There is only weak evidence for two or three transitions, namely of 361.8, 646.0, and 723.1 keV, in the 828.2-keV gate. In other gates where transitions of similar intensity are involved such as the 860.1-, 872.0-, and 960.8-keV gates, several transitions are clearly seen. The 960.8-keV gate exhibits many clear peaks. Thus, the 828.22-keV transition does not populate any level which has prompt  $\gamma$ -ray depopulation nor does it depopulate a level strongly fed by  $\gamma$  radiation. The only choice is that it feeds the isomeric 1013.79-keV level from a 1842.01-keV level. This level also allows the placement of three transitions that are seen weakly in the coincidence spectrum. The coincidence data suggest only about half the 646.00-keV transition intensity feeds this level. Since the coincidence statistics are poor and there is at present no alternative placement of this transition, all the 646.00-keV transition intensity is assigned as populating the 1842.01-keV level. While not shown in Table III, a limit of  $\alpha_K$  of the 828.22-keV transition restricts it to  $E1$  or  $E2$  multipolarity. Since essentially all the depopulation is to the  $\frac{13}{2}^+$  level with very weak transition to a  $\frac{9}{2}^+$  level, a tentative assignment of  $\frac{13}{2}^+$  is made for this level, too.

The 1965.9-keV level previously suggested<sup>4</sup> is now definitely confirmed by the 1043.8- and 688.5-keV gates where the 922.15- and 701.16-keV transitions, respectively, are seen for the first time. Based on  $\gamma$ -ray decays to  $\frac{5}{2}^-$ ,  $\frac{7}{2}^-$ , and  $\frac{9}{2}^-$  levels and a  $\log ft$  of 10.0, a spin and parity of  $\frac{7}{2}^-$  or  $\frac{9}{2}^-$  is allowed.

The spin of the 2252.3-keV level has been sug-

gested<sup>4</sup> to be  $\frac{9}{2}$ . Positive parity is established by the  $M1$  character of both the 493.65-keV transition to a  $\frac{9}{2}^+$  level and a 312.84-keV transition from a  $\frac{9}{2}^+$  level. In our coincidence data, a weak transition was observed to feed the 1264.77-keV,  $\frac{5}{2}^-$  level from this state. Thus, we conclude that the spin is  $\frac{7}{2}$ .

The 2488.16-keV level  $\gamma$  ray decays to  $\frac{7}{2}^-$ ,  $\frac{7}{2}^+$ ,  $\frac{9}{2}^+$ , and  $\frac{11}{2}^+$  states. These decays indicate a spin of  $\frac{9}{2}$  or  $\frac{7}{2}$ . Since there is also a transition to a possible ( $\frac{13}{2}^+$ ) level,  $\frac{7}{2}$  would be ruled out and  $\frac{9}{2}$  preferred; however, the  $\frac{13}{2}$  is not definite. The  $E2$  character of the 894.56-keV transition and  $M1$  character of the 235.97-keV transition establish even parity for the level.

The 2521.40-keV level previously suggested<sup>4</sup> is now definitely confirmed by the 703.4-1818.0- and (759-761)-1760-keV coincidence relations, as well as the 1764.3-757.1-keV coincidence. On the basis of decays to only  $\frac{5}{2}^-$  and  $\frac{7}{2}^-$  states and a  $\log ft$  of 8.3, a spin and parity of  $\frac{9}{2}^-$  and  $\frac{7}{2}^+$  is allowed.

## V. DISCUSSION

The level scheme of  $^{205}\text{Pb}$  based on the results of the present work is given in Fig. 5. There are some additional levels seen in the  $^{204}\text{Pb}(d, p)^{205}\text{Pb}$  and  $^{204}\text{Pb}(n, \gamma)^{205}\text{Pb}$  reaction studies.<sup>18,19</sup> A summary of all the energy levels in  $^{205}\text{Pb}$  and their spin and parity assignments known up to the present time is given in Fig. 6.

In 1967, Miranda<sup>20</sup> calculated the level structure of  $^{205}\text{Pb}$  using the shell model. A closed  $^{208}\text{Pb}$  core was assumed, and the three holes were distributed among the available neutron shells  $3p_{1/2}$ ,  $3p_{3/2}$ ,  $2f_{5/2}$ ,  $2f_{7/2}$ , and  $1i_{13/2}$ . The  $1h_{9/2}$  shell was omitted in these calculations, and phenomenological interaction was used. At that time, the calculated results were in reasonable agreement with the experimental results of Vegors, Heath, and Proctor.<sup>9</sup> However, the results of the present experiment are not in good agreement with Miranda's predictions.<sup>20</sup> As an example, there are many more negative-parity states than predicted in that work.

Very recently, a complete shell-model calculation has been performed for  $^{205}\text{Pb}$ , where a realistic two-body interaction was used.<sup>21</sup> The reaction matrix elements were deduced from the Hamada-Johnston potential according to the model of Kuo and Brown<sup>22</sup> and included the effects of core polarization. A closed  $^{208}\text{Pb}$  core was assumed, and the three holes were distributed among the six available neutron shells ( $3p_{1/2}$ ,  $3p_{3/2}$ ,  $2f_{5/2}$ ,  $2f_{7/2}$ ,  $1h_{9/2}$ , and  $1i_{13/2}$ ). The energies, spins, and parities that resulted from this calculation are given in Fig. 6



to be published; D. C. Camp, J. C. Manthuruthil, A. V. Ramayya, J. H. Hamilton, and J. J. Pinajian, *Bull. Am. Phys. Soc.* 15, 1649 (1970).

<sup>3</sup>D. C. Camp, V. Ananthakrishnan, A. Ramayya, J. Hamilton, J. Manthuruthil, and J. Pinajian, *Bull. Am. Phys. Soc.* 16, 492 (1971).

<sup>4</sup>T. D. Rupp and S. H. Vegors, Jr., *Nucl. Phys.* A163, 545 (1971).

<sup>5</sup>H. K. Carter and J. H. Hamilton, *Z. Physik* 235, 383 (1970).

<sup>6</sup>D. C. Camp, *Nucl. Phys.* A121, 561 (1968); D. C. Camp, in *Radioactivity in Nuclear Spectroscopy*, edited by J. H. Hamilton and J. C. Manthuruthil (Gordon and Breach, New York, 1972), p. 135.

<sup>7</sup>R. Gunnink, R. A. Meyer, J. B. Niday, and R. P. Anderson, *Nucl. Instr. Methods* 65, 26 (1968).

<sup>8</sup>J. T. Routti and S. G. Prussin, *Nucl. Instr. Methods* 72, 125 (1969).

<sup>9</sup>S. H. Vegors, Jr., R. L. Heath, and D. G. Proctor, *Nucl. Phys.* 48, 230 (1963).

<sup>10</sup>M. Schmorak, R. Stockendal, J. A. McDonell, and I. Bergström, *Nucl. Phys.* 2, 193 (1956/57).

<sup>11</sup>R. Stockendal and S. Hultberg, *Arkiv Fysik* 15, 33 (1959).

<sup>12</sup>R. Stockendal, *Arkiv Fysik* 17, 1076 (1960).

<sup>13</sup>K. E. Bergkvist and R. Stockendal, *Arkiv Fysik* 27, 25 (1964).

<sup>14</sup>R. S. Hager and E. C. Seltzer, *Nucl. Data* A4, 1 (1968).

<sup>15</sup>L. A. Sliv and I. M. Band, in *Alpha-, Beta-, and Gamma-ray Spectroscopy*, edited by K. Siegbahn (North-Holland, Amsterdam, 1965), p. 1639.

<sup>16</sup>M. R. Schmorak, *Nucl. Data* B6, 425 (1971).

<sup>17</sup>E. C. O. Bonacalza, P. Thieberger, and I. Bergström, *Arkiv Fysik* 22, 111 (1962).

<sup>18</sup>J. H. Bjerregaard, O. Hansen, O. Nathan, and S. Hinds, *Nucl. Phys.* A94, 457 (1967).

<sup>19</sup>E. T. Journey, H. T. Motz, and S. H. Vegors, Jr., *Nucl. Phys.* A94, 351 (1967).

<sup>20</sup>A. Miranda, *Nucl. Phys.* A92, 386 (1967).

<sup>21</sup>J. B. McGrory, private communication.

<sup>22</sup>T. T. S. Kuo and G. E. Brown, *Nucl. Phys.* 85, 40 (1966).

<sup>23</sup>K. L. Kosanke, W. C. McHarris, and W. H. Kelly, *Annual Report 1970-71, Cyclotron Laboratory, Michigan State University* (unpublished).

<sup>24</sup>M. Fujioka, private communication.